from 90 to 120 °C, and mesitylene-d_{12} was the solvent of choice from 120 to 140 °C. Above 140 °C decalin-d_{18} was used. The temperature ranges used to study the individual compounds are listed in Table I.

Concentration vs time data were analyzed by fitting the data to the dissociative kinetic model of this exchange shown in eq 4 using GIT software on a Vax 8650. This software is an iterative program based on the original HAVECHEM[32] programs. Eyring analysis of the kinetics data was done by using ARH2 software[33] on a Vax 8650. This version fits a logarithmic function to the data to avoid artifacts sometimes realized in linear fits of log data. RS/1 software was used to format the data into the expected inputs for these programs.

Synthesis of $^{13}CH_3PMe_3$. This compound was prepared in the drybox. $^{13}CH_3MgI$ was prepared by dissolving Mg into a dibutyl ether solution containing $^{13}CH_3I$. This solution was added to a cold dibutyl ether solution of PMe_2Cl and stirred for 30min as the solution warmed to ambient temperature. The resulting phosphine was distilled twice to remove all traces of butyl ether.

Synthesis of $P(CD_3)_3$. Perdeuteriotrimethylphosphine was prepared by adding a freshly prepared solution of CD_3MgI to tri-*p*-tolyl phosphite in dibutyl ether. The mixture was stirred for an hour at 25 °C, and the resulting phosphine was distilled at atmospheric pressure. The crude phosphine was redistilled to remove all traces of impurities.

Phosphine Exchange Kinetics. In the drybox a screw-capped Wilmad no. 507-Tr 5mm NMR tube was charged with 15–20 mg of $Cp^*(PMe_3)_2RuX$. Benzene-d_6 (approximately 600 μL) was added by pipette, and the tube was capped and reweighed. The entire assembly was cooled in a drybox freezer, along with a 100-μL syringe and $P(CD_3)_3$. After 30 min these items were removed from the freezer. The tube weight was rechecked, then $(P(CD_3)_3$ was added, by syringe, and the tube was reweighed. The total solution volume in the tube was determined by height.

The tube was placed in a preequilibrated 40 °C NMR probe and shimmed as thermal equilibrium was attained (approximately 15 min). Spectra were acquired, and the concentrations of species ($Ru-PMe_3$, $Ru-P(CD_3)_3$, PMe_3(soln), and $P(CD_3)_3$(soln) were determined over the same region of each spectrum by an automated series of GR and DR integration routines on the Nicolet spectrometers. The time of each spectrum was similarly recorded along with the data by the internal clock on the spectrometer. This concentration vs time data was simulated with GIT software to obtain the phosphine dissociation rate constant.

Dissociation rates of all th e ruthenium complexes at a variety of temperatures were measured by this same method.

Acknowledgment. We acknowledge the generous financial support of this work by the E. I. du Pont de Nemours and Co., Inc., the Shell Companies Foundation, and the National Science Foundation (Grant No. CHE-8600875). We wish to thank Dr. Don Tilley for carrying out some preliminary measurements of the rates of substitution for some of these compounds. We thank Drs. D. C. Roe and Peter Desrosiers for valuable discussions and assistance in obtaining accurate NMR data and gratefully acknowledge the technical assistance of Joseph H. McCartney and Joseph P. Foster, Jr.

Registry No. $^{13}CH_3PMe_2$, 117309-26-9; $P(CD_3)_3$, 22529-57-3; $^{13}CH_3I$, 4227-95-6; PMe_2Cl, 811-62-1; CD_3MgI, 41251-37-0; $Cp^*(PMe_3)_2Ru(N(C_6H_5)_2)$, 106734-56-9; $Cp^*(PMe_3)_2Ru(NHC_6H_5)$, 106734-55-8; $Cp^*(PMe_3)_2Ru(OH)$, 106734-52-5; $Cp^*(PMe_3)_2Ru(SC_6H_5)$, 117340-64-4; $Cp^*(PMe_3)_2Ru(OC_6H_5)$, 107441-18-9; $Cp^*(PMe_3)_2Ru(SH)$, 106734-57-0; $Cp^*(PMe_3)_2RuCl$, 87640-47-9; $Cp^*(PMe_3)_2Ru(CH_2Si(CH_3)_3)$, 87640-52-6; $Cp^*(PMe_3)_2RuBr$, 87640-48-0; $Cp^*(PMe_3)_2Ru(CH_2COCH_3)$, 106734-54-7; $Cp^*(PMe_3)_2RuI$, 93036-05-6; $Cp^*(PMe_3)_2Ru(C_6H_5)$, 107441-17-8; $Cp^*(PMe_3)_2Ru(CH_2C_6H_5)$, 117340-65-5; $Cp^*(PMe_3)_2Ru(CH_3)$, 87640-49-1; $Cp^*(PMe_3)_2Ru(C{\equiv}CC_6H_5)$, 106734-53-6; $Cp^*(PMe_3)_2RuH$, 87640-53-7; tri-*p*-tolyl phosphite, 620-42-8.

---

[32] Stabler, R. N.; Chesnick, J. *Int. J. Chem. Kinet.* **1978**, *10*, 461.

[33] Developed at DuPont by R. Farlee and D. C. Roe.

Multinuclear Magnetic Resonance Studies on Substituted Rhodium Carbonyl Clusters

Claudio Allevi, Silvia Bordoni, Charles P. Clavering, Brian T. Heaton,* Jonathan A. Iggo,* and Claudio Seregni

Department of Inorganic, Physical and Industrial Chemistry, University of Liverpool, P.O. Box 147, Liverpool L69 3BX, England

Luigi Garlaschelli

Istituto di Chimica Generale ed Inorganica, Università di Milano, Via G. Venezian 21, 20133 Milano, Italy

Received April 21, 1988

Multinuclear NMR data (^{13}C, ^{31}P, ^{103}Rh, $^{13}C\{^{103}Rh\}$, $^{13}C\{^{31}P\}$, and $^{31}P\{^{103}Rh\}$) for $[Rh_6(CO)_{12}\{P(OPh)_3\}_4]$, $[Rh_6(CO)_{10}(dppm)_3]$, and $(NBu_4)[Rh_6(CO)_{15}X]$ (X = I, CN, or SCN) are presented. The use of $^{13}C\{^{103}Rh\}$ double resonance has allowed the ^{13}CO NMR spectra of $[Rh_6(CO)_{15}I]^-$ and $[Rh_6(CO)_{12}\{P(OPh)_3\}_4]$ to be reassigned. The structures of the clusters in solution have been unambiguously determined. In all cases, the solid-state structure (as determined by X-ray crystallography) is maintained in solution. No evidence for CO exchange on the NMR time scale was found for any of the clusters studied at temperatures below 25 °C. ^{103}Rh NMR data for $[Rh_6(CO)_{15}X]^-$ (X = I, CN, SCN) are compared with those for $[Rh_6(CO)_{16}]$ and $[Rh_6(CO)_{15}H]^-$. Data for the phosphine-substituted derivatives of $[Rh_6(CO)_{16}]$ are compared with those for the ligand-substituted $[Rh_4(CO)_{12}]$ derivatives.

We have previously described the application of $^{13}C\{^{103}Rh\}$ NMR spectroscopy to the determination of the solution structures of $[Rh_4(CO)_{12-x}\{P(OPh)_3\}_x]$ (x = 1–4)[1] and of $[Rh_6(CO)_{15}H]^-$.[2] We now report multinuclear NMR, including $^{13}C\{^{103}Rh\}$ and $^{31}P\{^{103}Rh\}$, studies of Rh_6 clusters $[Rh_6(CO)_{15}X]^-$ (X = I, CN, SCN), $[Rh_6(CO)_{10}(dppm)_3]$, and $[Rh_6(CO)_{12}\{P(OPh)_3\}_4]$. These studies have allowed assignment of the ^{13}C, ^{31}P, and ^{103}Rh NMR spectra

---

[1] Heaton, B. T.; Strona, L.; Pergola, R. D.; Garlaschelli, L.; Sartorelli, U.; Sadler, I. H. *J. Chem. Soc., Dalton Trans.* **1983**, 173–175.

[2] Heaton, B. T.; Strona, L.; Martinengo, S.; Strumolo, D.; Goodfellow, R. J.; Sadler, I. H. *J. Chem. Soc., Dalton Trans.* **1982**, 1499–1502.

0276-7333/89/2308-0385$01.50/0

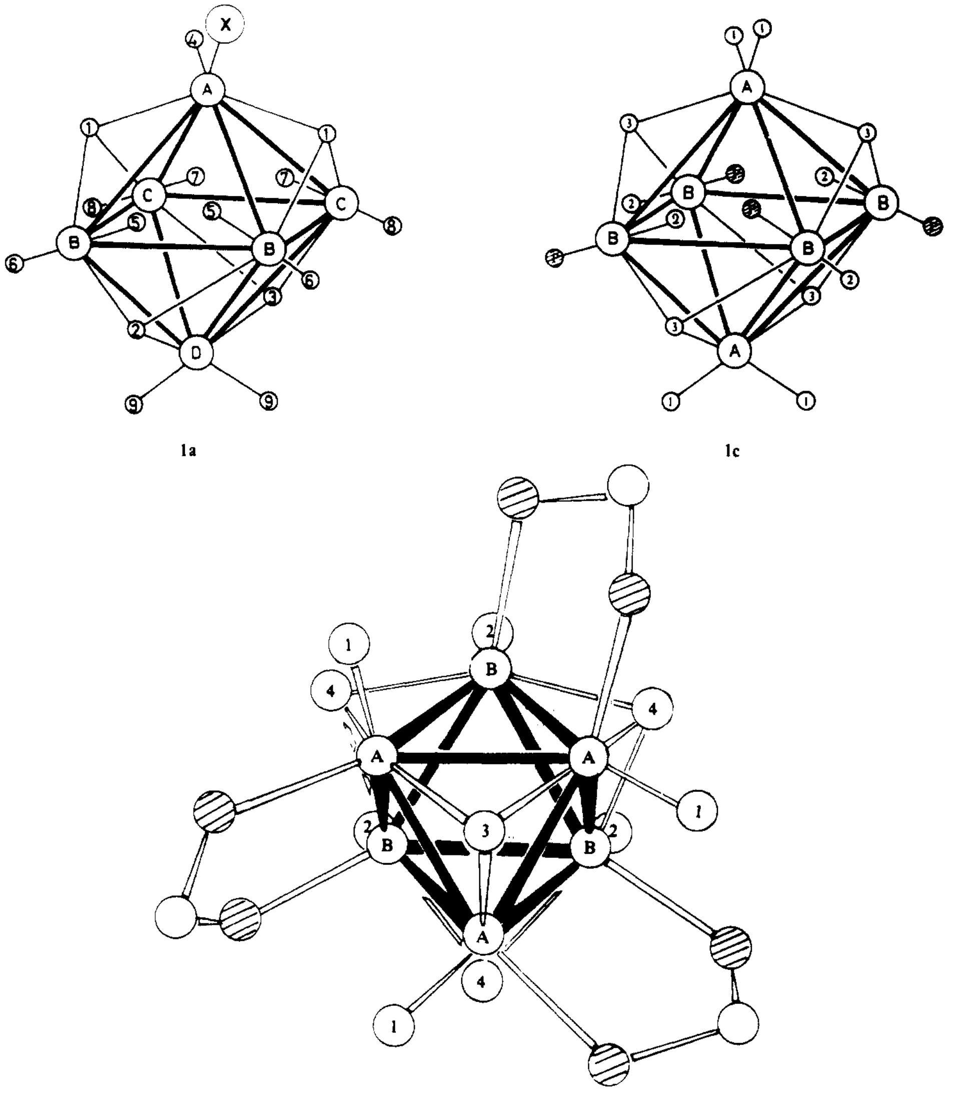

1a

1c

1b

Figure 1. Schematic representation of the structures of (a) $[Rh_6(CO)_{15}X]^-$, (b) $[Rh_6(CO)_{10}(dppm)_3]$ and (c) $[Rh_6(CO)_{12}\{P(OPh)_3\}_4]$ together with the atom labeling schemes.

which has enabled the structures in solution of the complexes to be established. The necessary probe modifications to allow observation of the ^{103}Rh-decoupled spectra on a Bruker WM200 spectrometer are described.

Results and Discussion

$[Rh_6(CO)_{15}X]^-$ (X = I, CN, SCN). The X-ray crystal structure of $[Rh_6(CO)_{15}I]^-$ has been reported.[3] A schematic representation of the structure, together with the CO and Rh labeling schemes used in this paper, is given in Figure 1a. The number of ^{103}Rh and ^{13}CO resonances expected for a structure of this type has been discussed previously.[2] Briefly, four rhodium resonances are expected and are found in the direct ^{103}Rh NMR spectrum (Table I). Three sets of resonances due to face-bridging carbonyls in the ratio 2:1:1 and six types of terminal carbonyls in the ratio 1:2:2:2:2:2 are predicted and observed. The ^{13}C NMR spectrum recorded at high resolution, which is significantly different to that reported previously,[4] is shown in Figure 2e, and the results of selective $^{13}C\{^{103}Rh\}$ measurements are shown in parts a–d of Figure 2. The spectroscopic data together with assignments are given in Table I.

Assignment of the rhodium and carbonyl-^{13}C resonances from the spectra in Figure 2 is straightforward. Thus, for example, irradiation of the rhodium nucleus resonating at 6.319458 MHz [$\delta(^{103}Rh)$ -91, -104 ppm][5] collapses the carbonyl doublet resonance of intensity 1 (C^4O in Figure 1a) at 185.3 ppm to a singlet and the multiplet of intensity 2 (assigned to C^1O) at 243.5 ppm to a doublet of doublets [$^1J(^{103}Rh_{B/C}-^{13}C^1O)$ = 17, 24 Hz]. This rhodium resonance can thus be unambiguously assigned to Rh_A (Figure 1a). Selective irradiation of Rh_B or Rh_C in order to assign the different rhodium–carbon coupling constants from $^{13}C\{^{103}Rh\}$ measurements was not possible because the resonance frequencies of Rh_B and Rh_C are so close together. We have, however, previously discussed the variation in $^1J(^{103}Rh-^{13}CO)$ with rhodium–carbon bond distance in $[NiRh_6(CO)_{16}]^{2-}$.[6] Data for several quite different clusters,

---

[3] Albano, V. G.; Bellon, P. L.; Sansoni, M. *J. Chem. Soc. A* **1971**, 678–682.

[4] Evans, J.; Johnson, B. F. G.; Lewis, J.; Matheson, T. W.; Norton, J. R. *J. Chem. Soc., Dalton Trans.* **1978**, 626–634.

[5] The first figure in parentheses is the rhodium chemical shift calculated from the $^{13}C\{^{103}Rh\}$ NMR experiment. The second figure is the rhodium chemical shift obtained from the direct ^{103}Rh NMR spectrum. The difference results from temperature effects (Table I).

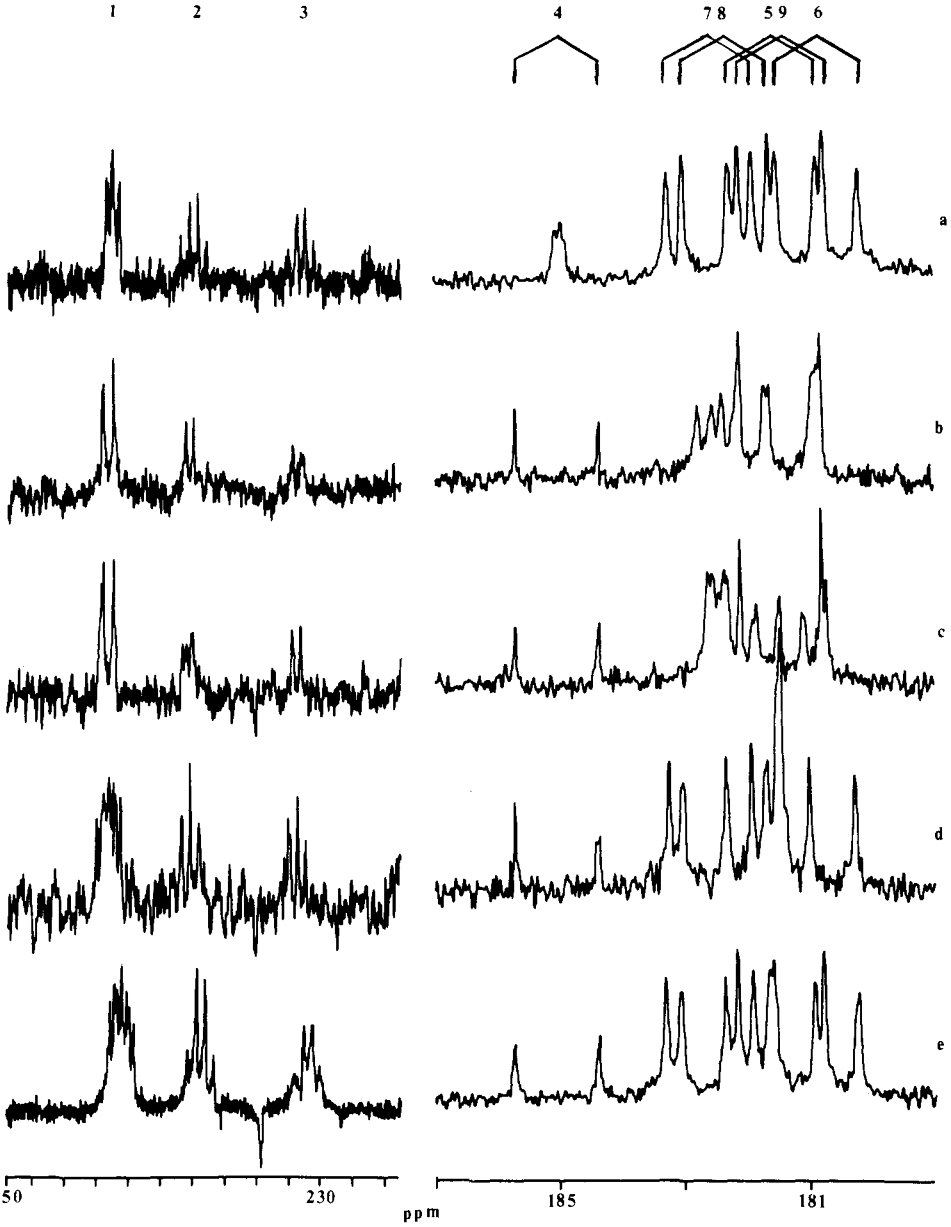

Figure 2. $^{13}CO\{^{103}Rh\}$ NMR spectra of $[Rh_6(CO)_{15}I]^-$: decoupling (a) Rh_A, (b) Rh_B, (c) Rh_C, (d) Rh_D; (e) fully coupled.

ranging from $[Rh_6(CO)_{15}I]^-$ to $[Rh_{10}As(CO)_{22}]^{3-}$, are presented in Figure 3. Although the scatter of points for terminal CO's is large, there is a surprisingly good correlation between $^1J(^{103}Rh-^{13}CO)$ and the bond distance for bridging carbonyl ligands. On this basis, we assign the 24-Hz coupling to $^1J(^{103}Rh_C-^{13}C^1O)$ [$d(Rh_C-C^1O)$ = 2.18 Å][3] and the 17-Hz coupling to $^1J(^{103}Rh_B-^{13}C^1O)$ [$d(Rh_B-C^1O)$ = 2.25 Å].[3] The unambiguous assignment of the resonances due to C^2O and C^3O (Figure 1a) is similarly made difficult. The assignment given in Table I could be reversed. The remaining ^{103}Rh and ^{13}C resonances of $[Rh_6(CO)_{15}I]^-$ are readily assigned from the $^{13}C\{^{103}Rh\}$ NMR measurements (Figure 2 and Table I) and are consistent with the structure found for the cluster in the solid state being maintained in solution. There was no evidence

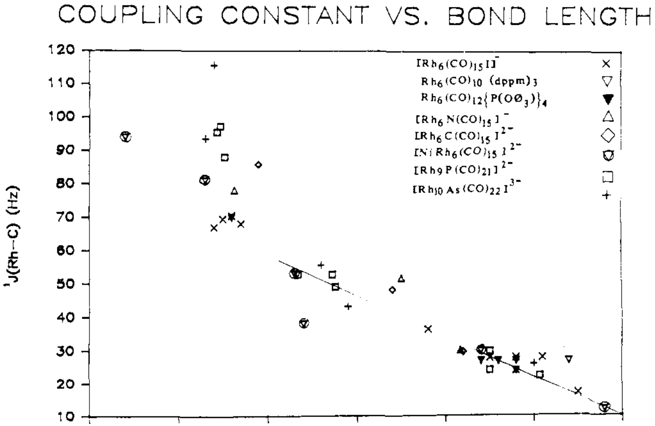

Figure 3. Variation in $^1J(^{103}Rh-^{13}C)$ with bond length for several rhodium–carbonyl clusters.

---

(6) Heaton, B. T.; Pergola, R. D.; Strona, L.; Smith, D. O.; Fumagalli, A. *J. Chem. Soc., Dalton Trans.* **1982**, 2553–2555.

(7) Heaton, B. T.; Strona, L.; Martinengo, S. *J. Organomet. Chem.* **1981**, *215*, 415–422.

(8) Bonfichi, R.; Ciani, G.; Sironi, A.; Martinengo, S. *J. Chem. Soc., Dalton Trans.* **1983**, 253–256.

(9) Vidal, J. L.; Walker, W. E.; Pruett, R. L.; Schoening, R. C. *Inorg. Chem.* **1979**, *18*, 129–136.

(10) Heaton, B. T.; Strona, L.; Pergola, R. D.; Vidal, J. L.; Schoening, R. C. *J. Chem. Soc., Dalton Trans.* **1983**, 1941–1947.

(11) Vidal, J. L.; Walker, W. E.; Schoening, R. C. *Inorg. Chem.* **1981**, *20*, 238–242.

Table I. NMR Spectroscopic Data for the Complexes

	assignmt	^{13}C $\delta^{a,b}$	assignmt	^{103}Rh $\delta^{c,d}$
$(NBu_4)[Rh_6(CO)_{15}I]$	C^1O	243.5 [ddd, J (Rh_AC) = 36.5, J (Rh_CC) = 24, J (Rh_BC) = 17]	Rh_A	−104
	C^2O	238.6 [dt, J (Rh_CC) = J (Rh_DC) = 28]^e	Rh_B	−405^e
	C^3O	231.8 [dt, J (Rh_BC) = J (Rh_DC) = 28]^e	Rh_C	−417^e
	C^4O	185.3 [d, J (Rh_AC) = 68]	Rh_D	−498
	C^7O	183.0 [d, J (Rh_CC) = 70]		
	C^8O	182.7 [d, J (Rh_CC) = 69]		
	C^5O	181.9 [d, J (Rh_BC) = 72]		
	C^9O	181.8 [d, J (Rh_DC) = 69]		
	C^6O	181.2 [d, J (Rh_BC) = 67]		
$(NBu_4)[Rh_6(CO)_{15}SCN]$	C^1O	241.5 [m]	Rh_A	148
	C^2O	236.6 [q, br]	Rh_B	−358^e
	C^3O	232.5 [q, br]	Rh_C	−403^e
	C^4O	185.3 [d, J (Rh_AC) = 70]	Rh_D	−460
	CO_t	184.6 [d, J (RhC) = 70]		
	CO_t	183.2 [d, J (RhC) = 73]		
$(NMe_3CH_2Ph)[Rh_6(CO)_{15}CN]$	μ-CO	ca. 236 [m]	Rh_A	−102
	CO_t	ca. 182 [m]	Rh_B	−430^e
	CN	135.9 [d, J (RhC) = 52]	Rh_C	−462^e
			Rh_D	−481
$[Rh_6(CO)_{10}(dppm)_3]^{f,g}$	C^3O	251.3 [m, br, J (Rh_AC) = 24]	Rh_A	−371^h
	C^4O	249.2 [dt, J (Rh_AC) = J (Rh_BC) = 27]	Rh_B	−152^h
	C^1O	188.2 [dm, J (Rh_AC) = 70]		
	C^2O	184.6 [dd, J (Rh_BC) = 70, J (PC) = 23]		
$[Rh_6(CO)_{12}\{P(OPh)_3\}_4]^i$	C^3O	244.3 [dt, J (Rh_BC) = 26.5, J (Rh_CC) = 19]	Rh_A	−296^j
	C^2O	185.1 [m, J (Rh_BC) = 68.7]	Rh_B	−418
	C^1O	184.8 [d, J (Rh_AC) = 70.4]		

[a] δ values are in ppm; J values in Hz. [b] Recorded in CD_3CN solution at 203 K. [c] 6.32 MHz = 0 ppm at such a magnetic field that the protons of TMS resonate at exactly 200 MHz. High-frequency (downfield) shifts are positive. [d] Recorded in $CD_3C(O)CD_3$ solution at 193 K. [e] Assignment could be reversed. [f] Recorded in $CDCl_3$ solution at 213 K. [g] ^{31}P NMR: δ 11.8 [d, br, $\sum J$ (Rh–P) = 128 Hz]. [h] Determined from the $^{13}C\{^{103}Rh\}$ NMR spectrum. [i] ^{31}P NMR: δ 108 [d, br, J (Rh–P) = 248 Hz]. [j] Recorded in $CDCl_3$ at 298 K.

for any fluxional process occurring on the NMR time scale between −80 and +30 °C. It should be noted that these measurements do not allow the relative orientation of the $\{Rh_A(C^4O)I\}$ fragment to be determined with respect to the remainder of the cluster, $\{Rh_5(CO)_{14}\}$, and the positions of C^4O and the iodine atom in Figure 1a must therefore be regarded as interchangeable.

We have also recorded the ^{13}C and ^{103}Rh NMR spectra for the analogous clusters $[Rh_6(CO)_{15}X]^-$ (X = CN, SCN) (Table I). The overall appearance of the ^{13}C and ^{103}Rh NMR spectra of the different complexes is similar and consistent with all the clusters adopting similar structures in solution. It is interesting to note that all three of these clusters show a ^{103}Rh resonance at high frequency (Table I), which we assign to the rhodium atom bearing the X ligand. This is further confirmed for $[Rh_6(CO)_{15}(^{13}CN)]^-$ in which the rhodium resonance at −102 ppm appears as a doublet—$^1J(^{103}Rh_A-^{13}CN)$ = 52 Hz. This contrasts with the resonance of the rhodium atom bonding to the hydride ligand in $[Rh_6(CO)_{15}H]^-$, which occurs at *lower* frequency than the other rhodium atom resonances in the cluster.[2] Although the effect of different ligands on the chemical shifts of metal nuclei are difficult to predict, a trend is emerging which shows that the hydride ligand produces an upfield shift of the rhodium resonance.[12]

$Rh_6(CO)_{10}(dppm)_3$. The crystal structure of $[Rh_6(CO)_{10}(dppm)_3]$ has been reported[13] and is shown schematically in Figure 1b. The cluster possesses a threefold rotation axis passing through C^3O (Figure 1b) and the centers of the Rh_A and Rh_B triangular faces. The faces defined by $(Rh_A)_3$ and $(Rh_B)_3$ are thus not equivalent. If this structure is maintained in solution, we would expect two multiplet resonances at different chemical shifts in the ^{31}P NMR spectrum, each showing coupling to rhodium, and four resonances in the ^{13}C NMR spectrum of relative intensities 3:3:1:3 corresponding to C^1O, C^2O, C^3O, and C^4O, respectively, in Figure 1b. The ^{31}P NMR spectrum of $[Rh_6(CO)_{10}(dppm)_3]$ has been reported previously[14] and shows a doublet of multiplets centered at 11.9 ppm with a doublet splitting of 130 Hz. In agreement with the literature, we find a broad doublet at 11.8 ppm with a splitting of 128 Hz. Furthermore, the spectrum is essentially invariant at all temperatures from −60 to +30 °C. If this was a simple (i.e. first-order) doublet, this might imply a fast, fluxional process that makes the Rh_A and Rh_B sites equivalent. However, we find the ^{31}P NMR spectrum collapses to a single broad line on irradiation at either 6.317669 MHz [δ(^{103}Rh) −371 ppm] or 6.319049 MHz (δ(^{103}Rh)−152 ppm] which clearly substantiates the nonequivalence of the rhodium triangles. We attribute these observations to second-order effects in the $(ABXY)_3$ (A, B = ^{31}P; X, Y = ^{103}Rh) 12-spin system of the $Rh_6(dppm)_3$ cluster core. The ^{31}P part of this spin system appears as a broadened doublet in the ^{31}P NMR spectrum. The 128-Hz splitting represents a sum of several rhodium–phosphorus couplings.

The ^{13}C NMR spectrum (in the carbonyl region) is, however, well-behaved (Figure 4) and is essentially invariant with temperature from −60 to +30 °C, indicating no fluxional behavior on the NMR time scale between these temperatures. The resonances observed are as expected for the structure found in the solid state being maintained in solution. $^{13}C\{^{103}Rh\}$ NMR measurements allow assignment of the carbonyl resonances which is given in Table I, based on the spectra in Figure 4. Shoulders on the resonances due to C^1O at 188.2 ppm indicate coupling to more than one phosphorus nucleus. Under Gaussian resolution ehancement, these resonances each split into quartets with $J(^{31}P-^{13}C)$ = 11.4 Hz indicating

---

(12) Ricci, J. S.; Koelzle, T. F.; Goodfellow, R. J.; Espinet, P.; Maitlis, P. M. *Inorg. Chem.* **1984**, *23*, 1828–1831.

(13) Ceriotti, A.; Ciani, G.; Garlaschelli, L.; Sartorelli, U.; Sironi, A. *J. Organomet. Chem.* **1982**, *229*, C9–C12.

(14) Foster, D. F.; Nicholls, B. S.; Smith, A. K. *J. Organomet. Chem.* **1982**, *236*, 395–402.

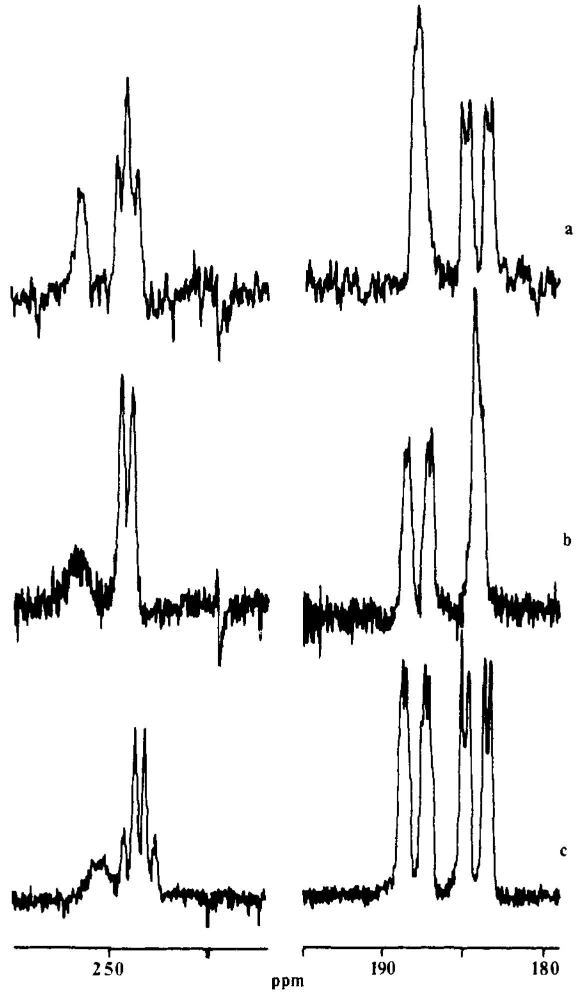

Figure 4. $^{13}CO\{^{103}Rh\}$ NMR spectra of $[Rh_6(CO)_{10}(dppm)_3]$: (a) Rh_A decoupled, (b) Rh_B decoupled; (c) fully coupled.

equal coupling to three phosphorus nuclei. Under the same resolution enhancement, the other terminal CO resonances at 184.6 ppm remain a clean doublet of doublets.

$Rh_6(CO)_{12}\{P(OPh)_3\}_4$. A schematic representation of the X-ray structure of $[Rh_6(CO)_{12}\{P(OPh)_3\}_4]$ is given in Figure 1c.[15] ^{13}C and ^{31}P NMR data for this complex have been previously reported.[16] Our data are reported in Table I and Figure 5 and differ from those in the literature. Thus, we find the phosphorus resonances to be at +108 ppm and not at −34.4 ppm as previously reported.[16] Our value for the doublet splitting, 248 Hz, is, however, in good agreement with the literature value of 250 Hz. This value for $^1J(^{103}Rh-^{31}P)$ corresponds closely with that found from the direct rhodium spectrum. Two groups of resonances are found in the direct $^{103}Rh-\{^1H\}$ NMR spectrum of relative intensity 1:2. The first of these, at −296 ppm, is a singlet and is assigned to the apical rhodium atoms, Rh_A in Figure 1c. The second resonance is a doublet centered at −418 ppm with a splitting of 248 Hz. This latter rhodium resonance is assigned to the equatorial rhodium atoms, Rh_B in the figure. As expected irradiation of this resonance collapses the doublet in the ^{31}P NMR spectrum to a singlet. We have previously reported the ^{103}Rh NMR spectra for the clusters $[Rh_4(CO)_{12-x}L_x]$ (x = 1–4). In agreement with the present work an upfield shift of the Rh resonances on substitution was observed.[1]

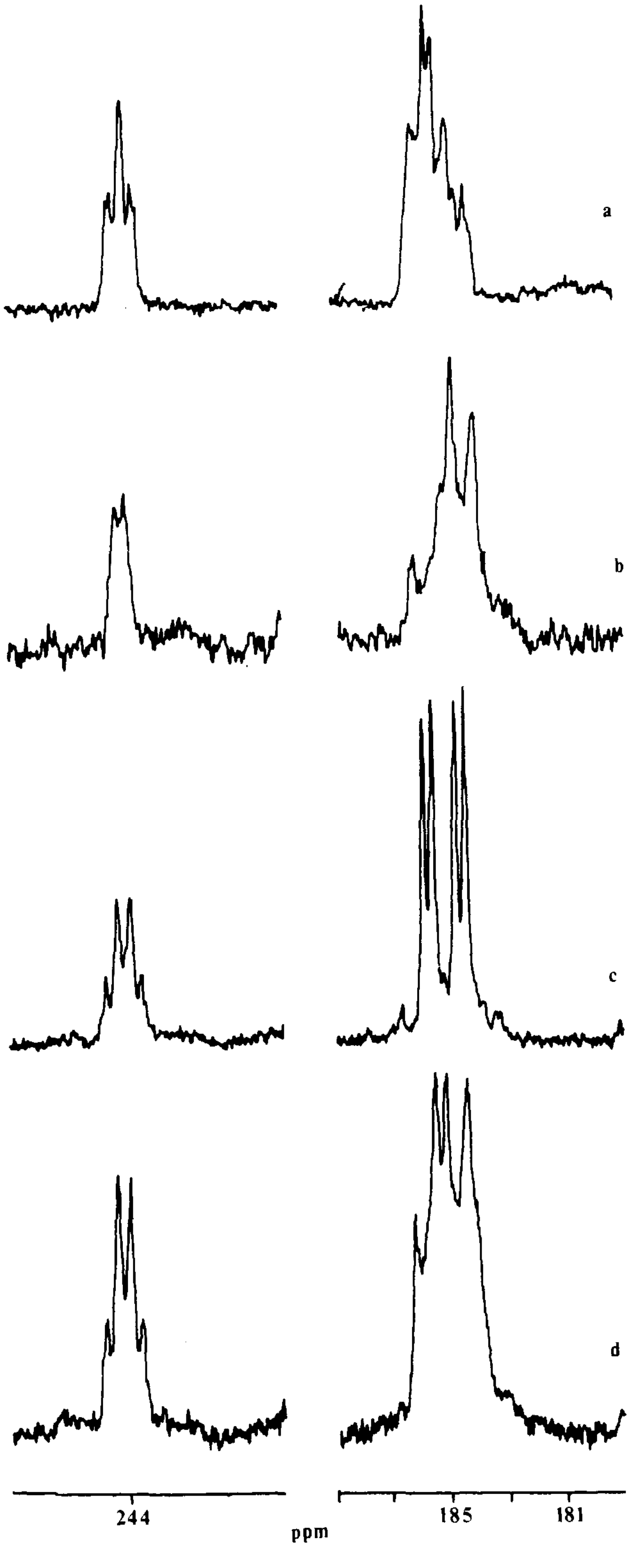

Figure 5. $^{13}CO\{X\}$ (X = ^{103}Rh, ^{31}P) NMR spectra of $[Rh_6(CO)_{12}\{P(OPh)_3\}_4]$: decoupling (a) Rh_A, (b) Rh_B, (c) P; (d) fully coupled.

It is generally observed in complexes of this type that long-range (greater than one bond) couplings between ^{103}Rh and ^{13}C and between ^{31}P and ^{13}C are small. Interpretation of the ^{13}C NMR spectrum can then usually assume first-order behavior since at the level of ^{13}C enrichment used (ca. 35%) $^{13}C-^{13}C$ coupling can be ignored. The ^{13}C NMR spectrum of $[Rh_6(CO)_{12}\{P(OPh)_3\}_4]$ is, however complicated by strong, long-range couplings in the equa-

---

[15] Ciani, G.; Manassero, M.; Albano, V. G. *J. Chem. Soc., Dalton Trans.* **1981**, 515–518.

[16] Abboud, W.; Taaritk, Y. B.; Mutin, R.; Basset, J. M. *J. Organomet. Chem.* **1981**, *220*, C15–C19.

torial plane of the Rh_6 cluster core. While it is possible to interpret the resonances and couplings associated with the carbonyl ligands of the apical Rh atom, Rh_A, on a first-order basis, this has not proved possible for the terminal carbonyl ligands of the equatorial Rh atoms, Rh_B. Thus irradiation at the frequency corresponding to Rh_A (Figures 1c and 5a) collapses the pseudo-first-order quartet in the ^{13}C NMR spectrum due to the bridging carbonyl ligands (C^3O) to a pseudo-first-order triplet and the resonances due to the directly bonded terminal carbonyl ligands (C^1O) to a singlet. However, while irradiation at the frequency corresponding to Rh_B collapses the resonances due to C^3O to a doublet, the behavior of the resonances due to the terminal carbonyls is complex. The quartet structure of the bridging CO resonances is thus seen to be due to accidental degeneracy of the couplings to the two different types of rhodiums, Rh_A and Rh_B, and not due to coupling to equivalent rhodium atoms as previously reported.[16] These couplings do not show the variation with the crystallographically determined Rh–C bond length found for the other clusters in Figure 3.

The behavior of the resonances in the ^{13}C NMR spectrum due to the terminal carbonyl ligands on Rh_B can be partially explained by consideration of the $^{13}C\{^{31}P\}$ NMR spectrum (Figure 5c). The $^{13}C\{^{31}P\}$ NMR spectrum in the terminal carbonyl region shows two doublets at 185.1 [$^1J(Rh_B{-}C^2O) = 68.7$ Hz] and 184.8 [$^1J(Rh_A{-}C^1O) = 70.4$ Hz]. The latter resonance appears essentially unchanged in the fully coupled ^{13}C NMR spectrum and can thus be assigned to the carbonyls on Rh_A, C^1O. We attribute the apparent line narrowing on phosphorus decoupling either to the removal of small long-range couplings or to accidental degeneracies with resonance lines of C^2O. The lower field doublet, however, appears as a multitude of poorly resolved lines in the fully coupled ^{13}C NMR spectrum. This poor resolution is not due to sample impurities, compare the cleanness of the $^{13}C\{^{31}P\}$ NMR spectrum of the same sample. We, therefore, attribute the poor resolution to long-range phosphorus–carbon couplings in the equatorial plane of the cluster. This contrasts with the situation we have previously found in $[Rh_4(CO)_{12-x}\{P(OPh)_3\}_x]$ ($x = 1$–4) where only a two-bond P–C coupling was observed.[1]

The ^{13}C, ^{31}P, and ^{103}Rh NMR data are thus seen to be consistent with the structure found in the solid state being maintained in solution. No evidence for fluxionality was found at temperatures in the range −60 to +30 °C.

Experimental Section

General experimental procedures were as described previously.[2] All compounds were prepared by literature methods.[13,15,17] NMR spectra were recorded on a Bruker WM200 (^{13}C, $^{13}C\{^{103}Rh\}$, and $^{31}P\{^{103}Rh\}$) or a Bruker WM250 ($^{13}C\{^{31}P\}$) instrument in Liverpool or through the SERC High Field NMR Service in Edinburgh on a Bruker WM360 instrument (^{103}Rh). External 85% H_3PO_4 was used as reference for ^{31}P NMR. The solvent resonances were used as reference for ^{13}C NMR. ^{103}Rh chemical shifts were referenced to 3.16 MHz = 0 ppm at such a field that the protons of TMS resonate at exactly 100 MHz. Chemical shifts are accurate to 0.1 ppm (^{13}C, ^{31}P) or 0.5 ppm (^{103}Rh). Coupling constants are accurate to 1 Hz. Decoupling frequencies were determined by monitoring the collapse of the ^{13}C or ^{31}P multiplets as previously described.[2]

Instrumentation

A 14-turn saddle coil wound from 20-gauge enameled copper wire and mounted on a glass former was placed outside the proton-decoupling coils of a standard Bruker broad-band probehead. The coil was tuned to the ^{103}Rh resonance frequency at 4.7 T (6.32 MHz) by using standard techniques.[18] The output from a Schlumberger digital signal generator Type FS30 amplified via a Marconi Instrument TF2167 broad-band radio frequency amplifier was used as the decoupling radiation. Problems with saturation of the IF stages of the receiver resulting from the closeness of the ^{103}Rh (6.32 MHz) and receiver intermediate (6.16 MHz) frequencies were largely overcome by the use of bandpass and bandstop filters in the irradiation and receive channels, respectively.[18]

Acknowledgment. We thank SERC for financial support (to C.A. and S.B.) and use of the high-field NMR service. We also thank CNR for supporting this work.

Registry No. $[Rh_6(CO)_{12}\{P(OPh)_3\}_4]$, 62863-23-4; $[Rh_6(CO)_{10}(dppm)_3]$, 83232-60-4; $(NBu_4)[Rh_6(CO)_{15}I]$, 32681-32-6; $(NMe_3CH_2Ph)[Ru_6(CO)_{15}CN]$, 38999-74-5; $(NBu_4)[Rh_6(CO)_{15}SCN]$, 38999-72-3; $[Rh_6(CO)_{15}I]^-$, 47778-52-9; $[NiRh_6(CO)_{16}]^{2-}$, 76774-51-1; $[Rh_6N(CO)_{15}]^-$, 84602-04-0; $[Rh_6C(CO)_{15}]^{2-}$, 54065-66-6; $[Rh_9P(CO)_{21}]^{2-}$, 68417-41-4; $[Rh_{10}As(CO)_{22}]^{3-}$, 75718-85-3; Rh, 7440-16-6.

---

(17) Chini, P.; Martinengo, S.; Giordano, G. *Gazz. Chim. Ital.* **1972**, *102*, 330–343.

(18) Fukushima, E.; Roeder, S. B. W. *Experimental Pulse NMR, A Nuts and Bolts Approach*; Addison-Wesley: Reading, MA, 1981; Chapter 5.